


# Characteristic properties of fly ash-based self-compacting geopolymer mortars with synthetic wollastonite microfiber produced from silica and calcite

 H.Ö. Öz,  D. Ünsal

Department of Civil Engineering, Niğde Ömer Halisdemir University (Niğde, Turkey)  
 [oznuroz@ohu.edu.tr](mailto:oznuroz@ohu.edu.tr)

Received 10 June 2022  
Accepted 02 December 2022  
Available on line 24 February 2023

**ABSTRACT:** This study investigated the fresh, physical, and mechanical properties of self-compacting geopolymer mortars (SCGs) with synthetic wollastonite microfiber (SWM). SCGs were designed with Class F fly ash (FA) as a binder by activating it with  $\text{Na}_2\text{SiO}_3$  and NaOH solutions. First, SWM was produced in the laboratory. Alkali ratios were determined as 1.5, 2.0, and 2.5, whereas SWM percentages were utilized as 0%, 4%, 8%, and 12% by weight of the binder. After geopolymer mortars were cured at 80 °C and 100 °C for 24 hours, respectively, they were kept at room temperature until testing age. The compressive strength, flexural strength, ultrasonic pulse velocity, dynamic modulus of elasticity, water sorptivity coefficient values, and physical characteristics of SCGs were tested at the end of the 28th day. The highest compressive strength value was obtained as 28.9 MPa for SCG-1.5-8 cured at 100 °C, while 6.5 MPa was measured as the highest flexural strength for SCG-2-12 cured at 80 °C.

**KEYWORDS:** Alkali ratio; Curing temperature; Self-compacting geopolymer; Synthetic wollastonite microfiber.

**Citation/Citar como:** Öz, H.Ö.; Ünsal, D. (2023) Characteristic properties of fly ash-based self-compacting geopolymer mortars with synthetic wollastonite microfiber produced from silica and calcite. *Mater. Construcc.* 73 [349], e307. <https://doi.org/10.3989/mc.2023.296322>.

**RESUMEN:** *Propiedades características de los morteros geopoliméricos autocompactantes a base de cenizas volantes con microfibras de wollastonita sintética producida a partir de sílice y calcita.* En este estudio se investigaron las propiedades físicas y mecánicas en estado fresco de los morteros de geopolímero autocompactante (SCG) con microfibras de wollastonita sintética (SWM). Los SCG se diseñaron con cenizas volantes (FA) de clase F como aglutinante y se activaron con soluciones de  $\text{Na}_2\text{SiO}_3$  y NaOH. En primer lugar, la SWM se produjo en el laboratorio. Las relaciones de álcalis quedaron determinadas como 1.5, 2.0 y 2.5, mientras que los porcentajes de SWM, como 0 %, 4 %, 8 % y 12 % en peso de aglomerante. Los morteros de geopolímeros se curaron a 80 °C y 100 °C durante 24 horas, respectivamente, y posteriormente se mantuvieron a temperatura ambiente hasta la edad de ensayo. Tras observar el diámetro de flujo de asentamiento de los SCG en estado fresco, a los 28 días se determinaron la resistencia a la compresión, la resistencia a la flexión, la velocidad del pulso ultrasónico y los valores del coeficiente de absorción de agua, así como las características físicas de los SCG. El valor de resistencia a la compresión más alto (28.9 MPa) se obtuvo para SCG-1.5-8 curado a 100 °C, mientras que 6.5 MPa se midió como la resistencia a la flexión más alta para SCG-2-12 curado a 80 °C.

**PALABRAS CLAVE:** Proporción de álcalis; Temperatura de curado; Geopolímero autocompactante; Microfibras de wollastonita sintética.

**Copyright:** ©2023 CSIC. This is an open-access article distributed under the terms of the Creative Commons Attribution 4.0 International (CC BY 4.0) License.

## 1. INTRODUCTION

The use of industrial aluminosilicate wastes or mineral admixtures, such as fly ash, silica fume, blast furnace slag, rice ask ash, metakaolin, glass powder, and marble powder, as cement replacement materials is favorable for reducing carbon dioxide emissions (1, 2). Thus, geopolymers, as an alternative to conventional concrete, produced by combining high quantities of silica and alumina are defined by a three-dimensional Si-O-Al chain structure (3). At the production stage, after the dissolution of aluminosilicate types within the alkaline medium, geopolymerization of the disintegrated ions into the temporary structural gel begins. Then, the ultimate hardening of the matrix is reached by the precipitation of the formed hydration products at the end of water vaporization and the development of crystalline structures. For example, the aluminum and silicon oxides in fly ash can react with alkaline liquids, such as sodium silicate ( $\text{Na}_2\text{SiO}_3$ ), sodium hydroxide (NaOH), potassium hydroxide (KOH), sodium aluminate ( $\text{NaAlO}_2$ ), potassium silicate, etc. Thus, a geopolymer that binds different size aggregates and other materials can be synthesized.

Type and activator concentration significantly affect fly ash dissolution due to the typical content of the activator improving the geopolymer's characteristics. Hardjito and Rangan (4) suggested that the geopolymer produced from a 14 M solution of NaOH resulted in a higher compressive strength than that of an 8 M solution of NaOH. The study by Abdullah *et al.* (5) found the maximum compressive strength of 7 days as 73.86 MPa when the ratio of  $\text{Na}_2\text{SiO}_3/\text{NaOH}$  was 2.5 at 70 °C for 24 hours. Moreover, Sanni and Khadiranaikar (6) reported that the workability of geopolymers increased with the increment in  $\text{Na}_2\text{SiO}_3/\text{NaOH}$  ratios used as 2.0, 2.5, 3.0, and 3.5. Due to a considerably slow geopolymeric reaction at ambient temperature, the heat curing process is another sensitive parameter affecting geopolymerization. Kürklü and Gorhan (7) studied the relationship between alkali solution concentration, curing time, and curing temperature on a fly ash-based geopolymer. They reported that 22 MPa was the highest compressive strength value of the geopolymer when 6M NaOH concentration was used at a curing temperature of 85 °C for 24 h at 28 days. However, Joseph and Mathew (8) found the maximum compressive strength of the geopolymer as 58 MPa at a curing temperature of 100 °C for 24 h at 28 days. Thus, a higher curing temperature can be attributed to the improvement of kinetic energy and the reaction degree that produces the geopolymer mortar with a stronger Al-Si-O network (9). Many researchers have performed studies on how to improve the strength characteristics of geopolymers.

One method is defined as adding fibers such as natural wollastonite (NW) and/or synthetic wollastonite

microfiber (SWM), reducing the propagation of microcracks in the material (10). Large reserves of NW are found in China, India, Finland, Mexico, Spain, the United States, Australia, and South Africa, accounting for most of the global SWM production. Turkey, Canada, Chile, Kenya, Namibia, Sudan, Tajikistan, and Uzbekistan are countries with significant NW resources (11). Synthetic wollastonite microfibers (SWMs), which have been previously produced in Turkey, have not been produced in our country for a long time. The annual average production amount of wollastonite in the world varies in the range of 500,000-600,000 tons. Due to its numerous unique properties, the use of NW and/or SWM has become more common in many application areas such as the plastic industry (37%), ceramic industry (28%), metallurgical industry (10%), paint industry (10%), friction products (9%), and other industries (9%) (12, 13).

SWM is an inert material that can be produced synthetically due to natural resources. Materials such as calcite ( $\text{CaCO}_3$ ) and quartz sand ( $\text{SiO}_2$ ), which are necessary to produce this mineral, are widely available in Turkey and other countries. However, although the extracted calcite is used in many sectors mentioned above, it is not used in the construction sector. In other words, using calcite as a mineral additive in structural applications adversely affects the strength characteristics of concrete (14). Moreover, calcite of color other than white is kept as a waste material in warehouses. Therefore, the production of SWM can contribute to the sustainable development of construction materials by enhancing the recycling of waste materials and reducing the use of cement (15). Öz and Güneş and Yücel and Özcan (15, 16) reported that the increased amount of SW did not increase or decrease  $\text{Ca(OH)}_2$  since it did not show a chemical reaction. This may be attributed to physical properties, such as the acicular particle structure and fine particle size distribution of SWM. Therefore, researchers have indicated that SW mineral have microfibers with the ability to bridge micro-cracks by achieving a higher load-carrying capability. Additionally, strength improvement can be explained by the formation of a function of the microfiber/matrix bond strength in the interfacial of SWM microfibers (15, 16).

Likewise, some studies in the literature (17) have explained the potential of natural (NW) or SWM for use as a reinforcing material over bridging microcracks and lagging formation of cracking. For example, Kalla *et al.* (18) reported that the compressive strength and flexural strength of concrete incorporating 15% of NW increased to 12% at 90 days because of the acicular morphology (fibrous nature) of wollastonite. Bong *et al.* (19) stated that using NW as a sand replacer in mixtures significantly improved flexural strength performance while compressive strength increased or remained unchanged. Moreover, the development of the microstructure of the geopoly-

mer matrix associated with additional wollastonite resulted in the increment of compressive strength (47.1 MPa). However, the wollastonite percentage increasing from 10% to 20% by mass led to a lower compressive strength (41.5 MPa) due to the weaker matrix resulting from the dysfunctional wollastonite particles based within the geopolymer matrix. In addition to the above-mentioned studies, literature studies showed that the flexural capacity of geopolymer matrix-reinforced samples increased due to NW partly melting in the alkaline medium and finally bound to the geopolymeric gel (20, 21). Thus, using wollastonite microfibers in structural design could result in an improvement of flexural strength due to its acicular morphology and filler effect. Moreover, Ransinchung and Kumar (22) found that the presence of NW mineral with a needle-shaped structure in the cement matrix reduced workability. Likewise, Bong et al. (19) indicated that workability decreased with the increasing wollastonite content in geopolymer mixtures with 0% (124 mm), 10% (107 mm), and 20% (100 mm) fiber percentages. Therefore, different solutions should be found to improve the workability of cementitious composites with wollastonite.

The self-compacting geopolymer/concrete design can decrease the workability-reducing effect of wollastonite. Self-compacting geopolymers (SCGs) are defined as a new type of geopolymers produced with various alkali activators, chemical additives, or the appropriate amount of water, not requiring any skills to succeed in the whole compaction process due to their high flowing consistency (23). Memon et al. (24) found the maximum compressive strength performance of a fly ash-based self-compacting geopolymer as 53.80 MPa using a 7% superplasticizer dosage at 28 days. Moreover, considering the influence of NW on the properties of SCGs, it was reported that the mechanical interlocking of unreacted NW molecules and binding to geopolymeric gel improved the microstructure of the geopolymer matrix (25). Likewise, Lee and Van Deventer (2) showed that soluble calcium released from NW could react quickly with Al and Si elements to develop the geopolymeric gel. When studies in the literature are reviewed without NW, there are three methods, the wet method, the liquid-phase reaction method, and the solid-state reaction method, to produce SWM (17). Considering the disadvantages of these production methods, SWM could be fabricated using a special production method developed by the researchers as a result of the sintering process. Thus, SWM can be replaced with NW used in the industrial field over time. According to the authors' knowledge, there are numerous studies on the effects of NW on geopolymer/concrete, while there is no literature on the impacts of SWM on SCGs. Therefore, partial replacement of the produced SWM with fly ash can be considered a friendly, sustainable solution for reducing the harmful effects of the cement production

industry on the environment. Moreover, using SWM instead of the main binder significantly improves the performance of cementitious composites due to its inert nature (16). Hence, using SWM instead of UK, the main binder of UK-based geopolymer, is a matter of interest. In fact, it will be an important scientific finding that SWM can provide a similar positive effect in geopolymers as cement-based composites.

This study aimed to determine the characteristic properties of self-compacting geopolymer mortars (SCGs) incorporating SWM. First, SWM with a high aspect/ratio (30:1) was designed under laboratory conditions using a special method. In the design of SCGs, alkali ratios ( $\text{Na}_2\text{SiO}_3/\text{NaOH}$ ) were chosen as 1.5, 2.0, and 2.5, while SWM percentages were utilized as 0%, 4%, 8%, and 12% by the weight of fly ash. The workability of SCGs was measured by the slump flow test. Then, SCGs were cured at 80 °C and 100 °C for 24 hours, respectively. Tests of compressive strength, flexural strength, ultrasonic pulse velocity, water sorptivity coefficient, and physical properties of SCGs were conducted at the end of the 28th day for the hardened state. This study reported on the development of novel SCGs incorporating SWM by using alkali activators under different curing conditions as a new construction material.

## 2. EXPERIMENTAL STUDY

### 2.1. Materials

SCGs were designed using Class F fly ash (FA) and alkaline activator solutions as binder materials in addition to SWM. Wollastonite, manufactured synthetically using lime (CaO) and silica ( $\text{SiO}_2$ ) raw materials, was used as a substitute for FA at certain ratios in the production of SCGs. The production methods of SWM consist of mechanochemical treatment, hydrothermal treatment, and a sintering process. First, CaO and  $\text{SiO}_2$  materials were mixed in a 1:1 mole ratio. The amount of pure water was calculated to be equal to the mixture's weight. The materials in the container were placed in the mill in such a way to prevent them from reacting. The mill was stirred at 250 rpm for 30 minutes to ensure mechanochemical interaction. After the mixture was added to Teflon, it was placed in an autoclave. The material was kept in the oven at 200 °C for 72 hours. The autoclave was removed from the oven after 72 hours and left to cool. After the hardened tobermorite (calcium silicate hydrate mineral) exploded in the microwave oven, it was removed from the Teflon by breaking with the help of a hammer. To vaporize the moisture from the material, it was kept in the oven at 100 °C for 20 hours. Then, the first grinding process of tobermorite was applied. After this process, the material was placed in porcelain containers, and sintering (the solid state reaction of

the production) was carried out at 1000 °C for 1 hour. As a result of the final grinding process, SWM with different aspect ratios was obtained. The aspect ratio can be defined as an image projection describing the proportional relationship between the width of an image and its height. At the end of the trial error methods, SWM with a high aspect ratio (the ratio of length to diameter) of 30:1 was fabricated for the design of SCGs under laboratory conditions using a special method. After scanning electron microscope (SEM) analysis, the acicular particle structure of SWM is presented in Figure 1. Chemical compositions of FA and SWM were examined in Table 1. The geopolymer binder was chemically activated by the alkaline solutions of NaOH and Na<sub>2</sub>SiO<sub>3</sub>. The ratio of Na<sub>2</sub>SiO<sub>3</sub> solution to NaOH solution was 1.5, 2.0, and 2.5 by weight of the binder. The composition of Na<sub>2</sub>SiO<sub>3</sub> solution comprised 25.4% SiO<sub>2</sub>, 14.7% Na<sub>2</sub>O, and 59.9% water by mass. Additionally, 13 M and 97% pure NaOH solution was utilized in the design. The alkali activators used are available locally. Alkaline solutions and water were the liquid components in all mixtures. Quartz aggregates with a 2.65 specific gravity (0–0.4 mm) were used as fine aggregates in the production of SCGs.

## 2.2. Mix proportions and casting

This study aimed to produce SCGs incorporating SWM by considering the alkali activator ratio and curing temperature. To this end, a total of 24 SCG mixtures were designed with different alkali ratios such as Na<sub>2</sub>SiO<sub>3</sub>/NaOH = 1.5, 2.0, and 2.5 and SWM replacement percentages specified as 0%, 4%, 8%, and 12% by weight of FA. Furthermore, the designed samples were cured at 80 °C and 100 °C, respectively. As seen in Table 2, the ratio of the alkaline solutions (Na<sub>2</sub>SiO<sub>3</sub>+NaOH) to the binder was designated as 0.5, as well as the binder content (1000 kg/m<sup>3</sup>) found by the sum of FA and alkaline solution. The sand/binder ratio was defined as 1.60. SWM with the aspect ratio of 30:1 obtained at the first stage of the study was utilized at the percentages of 0%, 4%, 8%, and 12% by weight of FA. Additionally, quartz aggregates (0–0.4 mm) were used in designing SCGs. The workability of fresh SCGs basically depends on the fundamental engineering properties of fresh SCGs with high performance characteristics. Therefore, the desired workability is a very important parameter for the design of SCGs. Thus, the slump flow test was

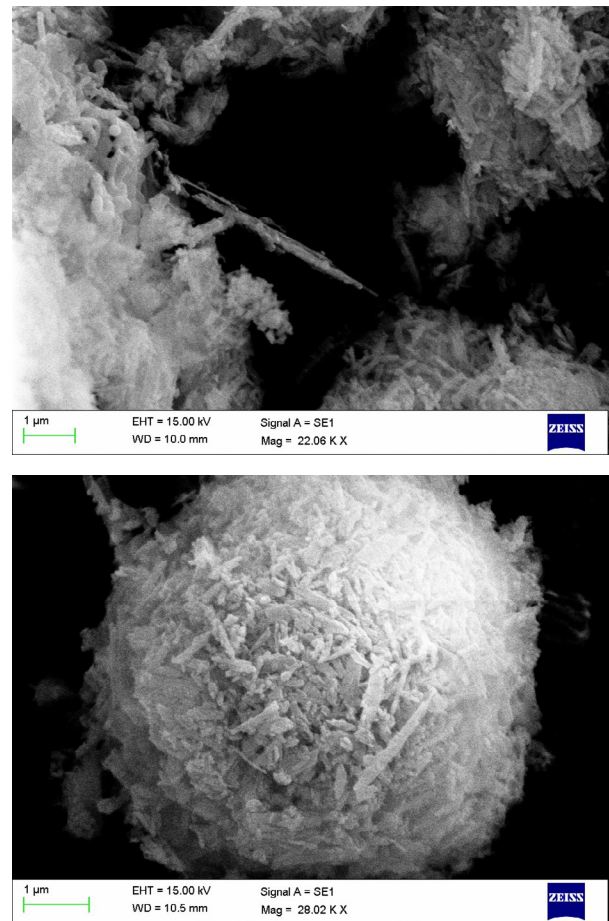


FIGURE 1. SEM analysis of SWM.

performed according to EFNARC guidelines (26), and the slump flow diameter of all SCGs was kept within the range of  $250 \pm 10$  mm. Hence, while producing the samples (considering the workability-reducing effect of SWM), the targeted slump flow diameter of SCGs was reached using different amounts of water without adding a high-range water-reducing admixture. First, a control mixture (SCG0) containing FA and quartz aggregates was produced without SWM. Then, SWM was used at the percentages of 4%, 8%, and 12% instead of FA and the different alkali activator ratios of Na<sub>2</sub>SiO<sub>3</sub>/NaOH determined as 1.5, 2.0, and 2.5 by weight, respectively. SCGs were named according to the percentage of SWM and alkali contents. For example, SCGs containing 4% SWM and 1.5 Na<sub>2</sub>SiO<sub>3</sub>/NaOH alkali ratio were called SCG1.5-4. In this way, SCG1.5-0, SCG1.5-4, SCG1.5-8, SCG1.5-12,

TABLE 1. Chemical composition and physical properties of FA and SWM.

Parameters (%)	CaO	SiO <sub>2</sub>	Al <sub>2</sub> O <sub>3</sub>	Fe <sub>2</sub> O <sub>3</sub>	MgO	SO <sub>3</sub>	K <sub>2</sub> O	Na <sub>2</sub> O	TiO <sub>2</sub>	LOI	Specific Gravity
Fly Ash	1.47	61.25	22.19	7.02	1.7	0.06	2.34	0.27	0.9	2.60	2.31
Synthetic Wollastonite Microfiber	45.689	52.613	0.429	0.18	0.266	-	0.093	0.142	-	-	2.82

SCG2-0, SCG2-4, SCG2-8, SCG2-12, SCG2.5-0, SCG2.5-4, SCG2.5-8, and SCG2.5-12 mixtures were obtained at different curing temperatures.

Various ingredients and production processes can be used to produce geopolymers. Various synthesis routes are mixed and reacted with an aluminosilicate precursor to commence the polymerization process. Therefore, there are no standard procedures for geopolymer production (27). The geopolymer mixing procedure consisted of dry and wet mixing. The solid components of SCGs (FA, quartz aggregates, and SWM) were in the mixer for about 30 sec as a dry condition. The liquid ingredients of the mixture, i.e., the sodium silicate solution, the sodium hydroxide solution, and water, had been previously mixed with each other in a container before adding to the dry mix. Then the dry mixing and the wet mixing continued for another 4 min.

Slump flow diameters were measured on fresh SCGs. According to the specifications of EFNARC (26), the slump flow diameter for SCGs should change between 24-26 cm. Therefore, many trial mixtures were produced until the target slump flow diameter was reached without using a high-range water-reducing admixture. Then, SCGs were cured in the oven at 80 °C and 100 °C for 24 h. After the curing process, the samples were demolded and kept at room temperature (23±2 °C) to be tested until the 28th day. Compressive strength, flexural strength, UPV, water sorptivity coefficient, and various physical properties were measured for SCGs incorporating SWM at the end of the 28th day.

### 2.3. Test procedures

#### 2.3.1. Slump flow diameters

The slump flow diameter for SCGs should be kept within the range of 24-26 cm according to EFNARC guidelines (26). The slump flow diameter values of fresh SCGs were calculated by a mini settling funnel with a truncated cone shape. The slump flow diameter was measured by reading more than two vertical direction diameters and taking their average.

#### 2.3.2. Physical properties

The physical properties of the mortars were determined according to ASTM C642-13 standard (28) using 40x40x160 mm prismatic specimens on the 28th day. The test steps were as follows: weighing air dry weights (W3), keeping the samples in the water tank for 24 h, measuring their weight after drying their surfaces with a napkin (W4), weighing the samples for the Archimedes scale experiment in water (W2), and measuring the samples' weight by keeping them in an oven at 100 °C for 24 h (W1). The hardened bulk density, dry specific gravity, apparent specific gravity, saturated dry surface specific gravity, water absorption, and apparent porosity values of SCGs were determined on the 28th day. The test measurements were performed by taking the average values of 3 samples.

$$\text{Hardened Bulk Density} = \frac{w1}{v} \quad [1]$$

$$\text{Dry Specific Gravity} = \frac{w1}{w4-w2} \quad [2]$$

TABLE 2. Mix proportions of SCGs (kg/m<sup>3</sup>).

Code	Groups	Alkali ratios	Synthetic Wol-lastonite (%)	Fly Ash	Synthetic Wol-lastonite Microfiber	Aggregate	Na <sub>2</sub> SiO <sub>3</sub>	NaOH	Water
SCG1.5-0	I	1.5	0	666.6	0	1062.0	200.0	133.3	83.8
SCG1.5-4			4	640	26.6	1067.9	200.0	133.3	107.9
SCG1.5-8			8	613.3	53.3	1073.7	200.0	133.3	107.9
SCG1.5-12			12	586.6	80	1080	200.0	133.3	128.8
SCG2-0	II	2	0	666.6	0	1059.2	222.2	111.1	89
SCG2-4			4	640	26.67	1065.3	222.22	111.11	90.5
SCG2-8			8	613.34	53.33	1071	222.22	111.11	90.5
SCG2-12			12	586.67	80	1076.8	222.22	111.11	93.3
SCG2.5-0	III	2.5	0	666.67	0	1057.22	238.1	95.24	87
SCG2.5-4			4	640	26.67	1063	238.1	95.24	92.5
SCG2.5-8			8	613.34	53.33	1068.9	238.1	95.24	92.5
SCG2.5-12			12	586.67	80	1074.6	238.1	95.24	92.5

$$\text{Apparent Specific Gravity} = \frac{w_1}{w_1 - w_2} \quad [3]$$

$$\text{Saturated Dry surface Specific Gravity} = \frac{w_4}{w_4 - w_2} \quad [4]$$

$$\text{Water Absorption} = \frac{w_4 - w_1}{w_1} \times 100 \quad [5]$$

$$\text{Apparent Porosity} = \frac{w_3 - w_1}{w_3 - w_2} \times 100 \quad [6]$$

### 2.3.3. Compressive strength, flexural strength, UPV, and dynamic modulus of elasticity

According to ASTM C348-14 standard (29), the flexural strengths of 3 prismatic samples with the dimensions 40x40x160 mm were measured using a device with a loading speed of 0.05 kN/s on the 28th day. In line with ASTM C349-14 standard (30), six broken cubic samples with dimensions 40 mm obtained from the flexural strength test were used to calculate compressive strength values. The loading speed for compressive strength was 2.4 kN/s.

The ultrasonic pulse velocity (UPV) test, a non-destructive testing method, is a very common technique in civil engineering. This test can assess the relative quality of composites and their defects (voids, cracks, the effectiveness of their repair, etc.). In this test, the transit time of ultrasonic pulses was measured with 50–58 kHz created by an electroacoustical transducer, passing from one side of the specimen to the opposite. The ultrasonic pulse velocity (UPV) test was conducted in line with ASTM C597-16 standard (31) using a 160 mm length of the samples on the 28th day.

Meanwhile, the dynamic modulus of elasticity was calculated based on the equation indicated by the researchers below (32):

$$\text{DME} = \rho \times v^2 \quad [7]$$

Where DME is the dynamic modulus of elasticity (MPa),  $\rho$  is the concrete density ( $\text{kg}/\text{m}^3$ ), and  $v$  is the ultrasonic pulse velocity (m/s).

The mechanical characteristics of geopolymer mortars were obtained by calculating the average of three samples used in each test. The average values of the three samples were calculated when determining all mechanical values.

### 2.3.4. Water sorptivity coefficient

The 70x70x70 mm-sized samples prepared for the water sorptivity test were kept in the oven at 80 °C and 100 °C for 24 hours on the 28th day to remove the water inside them before the test. Then paraffin was applied to the junction of the four corners of a surface so that only one surface could contact water. The water sorptivity coefficient values of the samples were

measured in a ball pool containing 5 mm deep water in accordance with ASTM C1585-20 standard (33). After measuring their first weight, the samples were placed in water. Then, the samples were removed from the water to measure their weights at the first, fourth, ninth, sixteenth, twenty-fifth, thirty-sixth, forty-ninth, and sixty-fourth minutes. According to the test procedure, results were calculated with the determined average of the 3 samples' values using the equation below:

$$I = S^1 \sqrt{t} \quad (17, 33) [8]$$

Where  $S^1$ : sorptivity ( $\text{mm}/\text{min}^{1/2}$ ),  $I$ : cumulative infiltration (mm), and  $t$ : time (min).

## 3. RESULTS AND DISCUSSION

### 3.1. Slump flow diameters

As observed from Figure 2, SCGs were produced with a slump flow diameter determined as  $25.0 \pm 1.0$  cm. All SCGs designed in this study were manufactured without any segregation, as shown in Figure 3. The slump flow diameters of SCGs were very close to each other. The desired workability was obtained by adding water determined as 83.8, 107.9, 107.9, and 128.8  $\text{kg}/\text{m}^3$  for SCG1.5-0, SCG1.5-4, SCG1.5-8, and SCG1.5-12, respectively. Therefore, as seen in Figure 2 and Table 2, the slump flow diameter for the desired workability was increased by increasing the amount of SWM due to the excessive amount of water. The slump flow diameters of SCGs decreased with the increasing amount of SWM. For example, it was evident from Figure 2 that although the same amount of water was used in the mixtures such as SCG-2.5-4 and SCG-2.5-12, the slump flow diameter decreased from 25.6 to 24.8 cm due to the needle-like particle structure of SWM. The decreased workability of geopolymer mortars with the addition of SWM can be explained by the increased bonding of SWM microfibers. Therefore, as the usage percentage of SWM was increased, the required amount of water for the aimed slump flow diameter of SCGs also increased. Similarly, to these results, Tatnall (34) indicated that the increased interlocking effect due to the needle-like structure of SWM reduced the workability of the mixture and thus, additional water and/or plasticizers should be used. Moreover, the amount of water needed for the same workability decreased due to the increment of water in SCGs with the increasing  $\text{Na}_2\text{SiO}_3/\text{NaOH}$  ratio. For example, as seen in Table 2, the amount of water was changed to 128.85, 93.3, and 92.5  $\text{kg}/\text{m}^3$  for SCG1.5-12, SCG2.0-12, and SCG2.5-12 mixtures, respectively. The reason for this is thought to be the amount of water for a 2.5 alkali ratio in SCGs higher than a 1.5 alkali ratio due to the 59.9%  $\text{H}_2\text{O}$  contained in  $\text{Na}_2\text{SiO}_3$  (6).



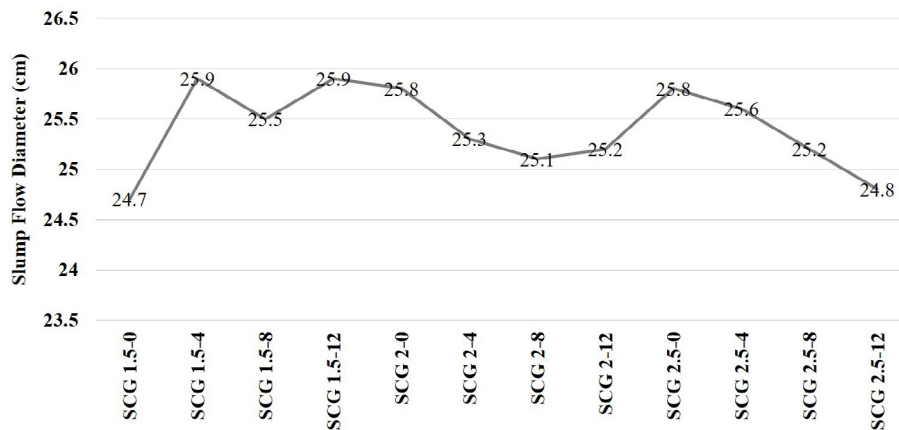


FIGURE 2. Slump flow diameter results.

### 3.2. Physical properties

SWM, the alkali activator ratio, and the curing temperature of geopolymer mortars substantially affected the physical properties of SCGs. As shown in Tables 3 and 4, the highest hardened bulk density value cured at 80 °C (1905 kg/m<sup>3</sup>) and the lowest hardened bulk density value (1637 kg/m<sup>3</sup>) cured at 100 °C were obtained from SCG-2-0 and SCG-2.5-12, respectively. When certain percentages of SWM were used instead of FA with high-dimensional particles serving as a filler, the void ratio increased due to the water leaving the sample, and the hardened bulk density values of the groups generally decreased. This was also supported by Patankar et al. (35). Upon comparing the curing temperatures, it was revealed that the hardened bulk density values of the samples cured at higher curing temperatures were relatively lower, which was explained by the fact that more water left the sample at higher temperatures. Additionally, it was observed that when the amount of SWM was increased for SCG 1.5 (Group I) mortars cured at 100 °C, the hardened bulk density values of SCGs increased on the 28th

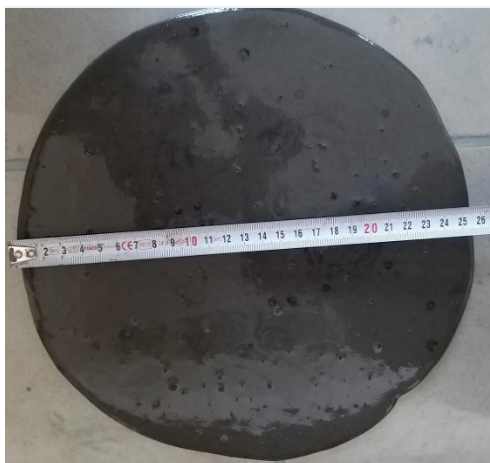


FIGURE 3. Measuring the slump flow diameter.

day, and this improvement proceeded to 8% of SWM (including 8%). This may be attributed to the optimum amount of FA, alkali ratio, binder, and water for a better design. Thus, substituting SWM with FA resulted in the intensified matrix structure of SCGs. However, using SWM at a 12% level reduced the physical performance of SCGs, which was clarified by the weakened bond in the matrix (15). Considering hardened bulk density values, the SCGs produced in this study can be classified as a structural lightweight material.

The dry specific gravity, apparent specific gravity, and saturated dry surface specific gravity values of SCG mortars obtained from the experiments performed on the 28th day under different curing conditions are also presented in Tables 3 and 4, respectively. According to the test results, the dry specific gravity values of SCGs were in the range of 1.73-1.89, apparent specific gravity values changed between 2.33-2.51, and saturated dry surface specific gravity values varied between 2.00-2.12. Additionally, a decrease was observed in apparent specific gravity and saturated dry surface specific gravity values with the decrease in the amount of NaOH in the mortar in the comparison of Groups I and II (36). This may be attributed to the lower quality geopolymer of the matrix controlled by the lowest alkaline ratio, responsible for the insufficient dissolution of solid fly ash particles. It can be noted that using an excessive amount of alkaline activator solution for Group III resulted in a little expansion of geopolymer mortars during the reaction (37). Moreover, the lower initial water content would result in a denser microstructure (38).

Figure 4 and Figure 5 indicate the measurement of water absorption and apparent porosity values for geopolymer mortars with different design parameters on the 28th day. According to the test results, the water absorption values of geopolymer mortars were in the range of 8.10-13.82%, and apparent porosity values changed between 5.90-24.00%. The highest water absorption and apparent porosity values were

TABLE 3. Hardened bulk density, dry specific gravity, apparent specific gravity, and saturated dry surface specific gravity of SCGs cured at 80 °C (kg/m<sup>3</sup>).

Code	Hardened Bulk Density	Dry Specific Gravity	Apparent Specific Gravity	Saturated Dry Surface Specific Gravity
SCG1.5-0	1.85	1.84	2.50	2.08
SCG1.5-4	1.81	1.83	2.49	2.07
SCG1.5-8	1.79	1.82	2.46	2.06
SCG1.5-12	1.75	1.81	2.43	2.04
SCG2-0	1.90	1.89	2.51	2.11
SCG2-4	1.89	1.84	2.47	2.07
SCG2-8	1.84	1.81	2.47	2.06
SCG2-12	1.73	1.79	2.46	2.06
SCG2.5-0	1.90	1.89	2.49	2.11
SCG2.5-4	1.84	1.79	2.44	2.03
SCG2.5-8	1.81	1.78	2.42	2.01
SCG2.5-12	1.78	1.76	2.40	2.00

TABLE 4. Hardened bulk density, dry specific gravity, apparent specific gravity, and saturated dry surface specific gravity of SCGs cured at 100 °C (kg/m<sup>3</sup>).

Code	Hardened Bulk Density	Dry Specific Gravity	Apparent Specific Gravity	Saturated Dry Surface Specific Gravity
SCG1.5-0	1.76	1.75	2.40	2.06
SCG1.5-4	1.78	1.76	2.40	2.02
SCG1.5-8	1.80	1.81	2.41	2.01
SCG1.5-12	1.75	1.75	2.33	1.99
SCG2-0	1.82	1.85	2.48	2.09
SCG2-4	1.79	1.83	2.43	2.05
SCG2-8	1.70	1.80	2.42	2.05
SCG2-12	1.69	1.72	2.33	1.98
SCG2.5-0	1.84	1.83	2.46	2.07
SCG2.5-4	1.80	1.78	2.41	2.05
SCG2.5-8	1.80	1.76	2.38	2.04
SCG2.5-12	1.63	1.72	2.36	2.03

obtained from SCG-1.5-12 cured at 80 °C, whereas the lowest values were measured from SCG-1.5-8 cured at 100 °C. Furthermore, an increase in the porosity and water absorption rate was observed for all groups at both curing temperatures, except for SCG-1.5 cured at 100 °C. The increment of the liquid to solid percentage enhanced the dissolution of aluminosilicate resource by facilitating the ion transference (39), which led to slower polycondensation reactions, resulting in the transformation of a few meshes. Additionally, a higher amount of water remaining in the geopolymer matrix caused a reduction in physical properties. Moreover, the porosity of SCGs advanced due to the formation of more than

one network and the amount of water trapped in the geopolymer matrix (40). However, a decrease in water absorption and apparent porosity was observed in SCG-1.5 cured at 100 °C. It was thought that curing at high temperatures increased the degree of geopolymerization and contributed to the formation of a denser material, which reduced the water absorption and apparent porosity values of geopolymer mortars (41). SWM also decreased pores in the geopolymer matrix and water absorption and apparent porosity due to the filler effect by providing the condensation of the microstructure, which ensured pore discontinuity in the geopolymer matrix for Group I at high curing temperatures (22, 23, 42). Therefore, it was



stated that SWM, defined as an inert material not reacting chemically in the pore solution, affected the formation of the pore network tortuosity of SCGs (43). However, this improvement was not observed in Groups II and III at lower and higher curing temperatures. The deterioration of water absorption and apparent porosity may be attributed to the attenuation of the matrix bond in the interfacial transition zone of SWM due to the insufficient alkali ratio and curing temperature required for the best geopolymerization for SCGs (15).

### 3.3. Compressive strength, flexural strength, UPV and dynamic modulus of elasticity

The compressive and flexural strength values of SCGs are graphically presented in Figures 6 and 7, respectively. As seen from Figure 6, the compressive strength values of geopolymer mortars were in

the range of 12.8-28.9 MPa. The highest compressive strength was obtained from SCG-1.5-8 cured at 100 °C, while SCG-1.5-12 cured at 80 °C had the lowest compressive strength.

In the development of SCGs, curing temperature, alkali activator ratio, and the replacement percentage of SWM played an important role during the activation process. As seen from Figure 6, the compressive strength values of the samples cured at 100 °C in each of Group I, Group II, and Group III were higher than those of the samples cured at 80 °C. Curing at high temperatures increased the degree of geopolymerization and contributed to the formation of a denser material (41). As indicated in Figure 6, when the samples cured at 80 °C were compared, it was determined that the compressive strength values of Group I were lower than those of Group II and Group III, respectively. It is thought that the reason for this was the decreased amount of  $\text{Na}_2\text{SiO}_3$ , which contains 59.9% water. On the other hand, the growth rate of compressive strength at higher curing temperatures can be explained by the

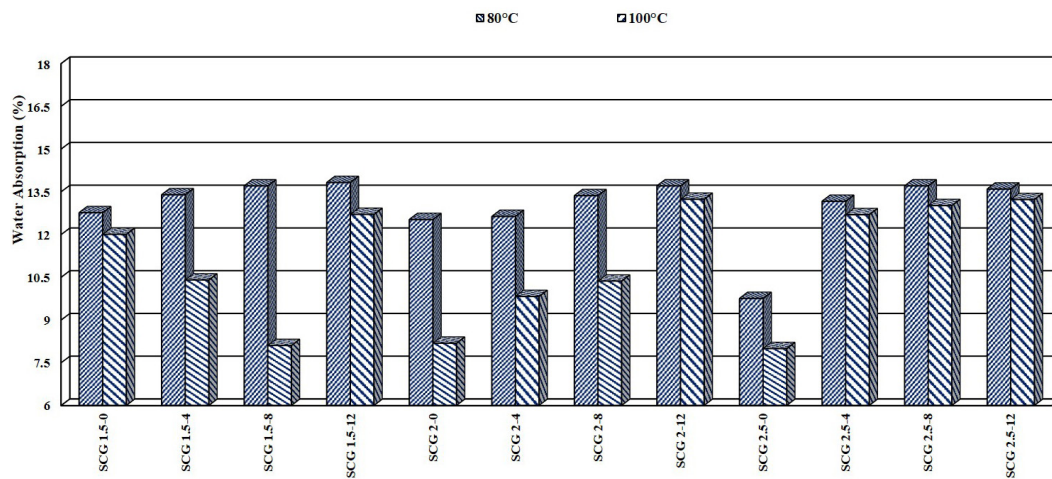


FIGURE 4. Water absorption values of SCGs cured at 80 °C and 100 °C.

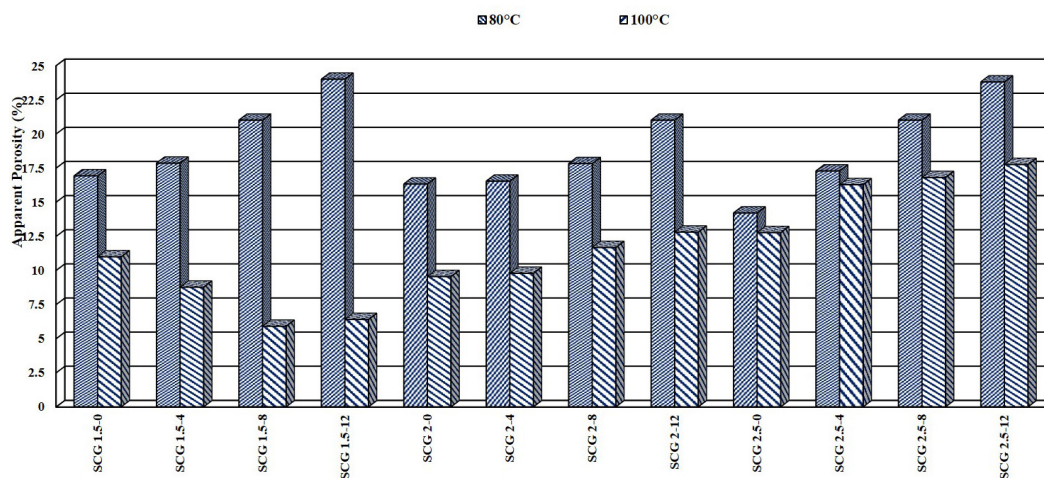


FIGURE 5. Porosity values of SCGs cured at 80 °C and 100 °C.

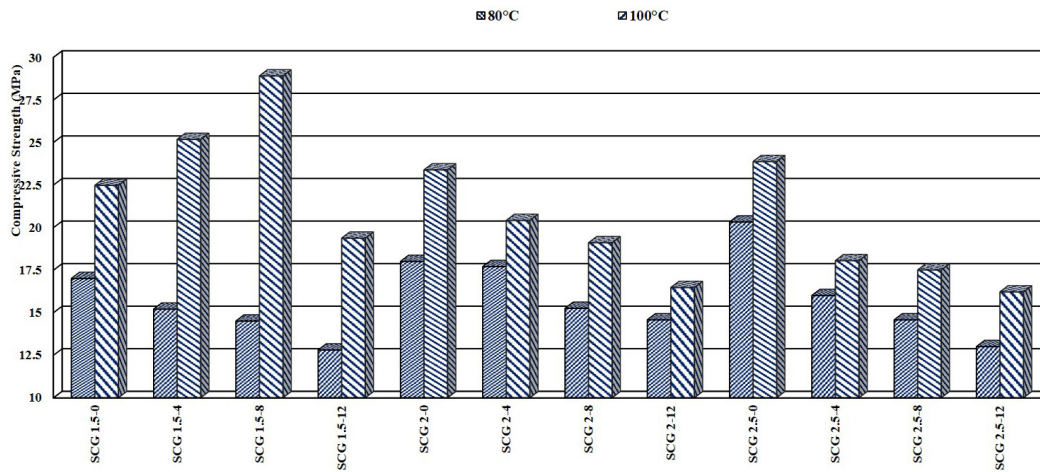


FIGURE 6. Compressive strength values of SCGs cured at 80 °C and 100 °C.

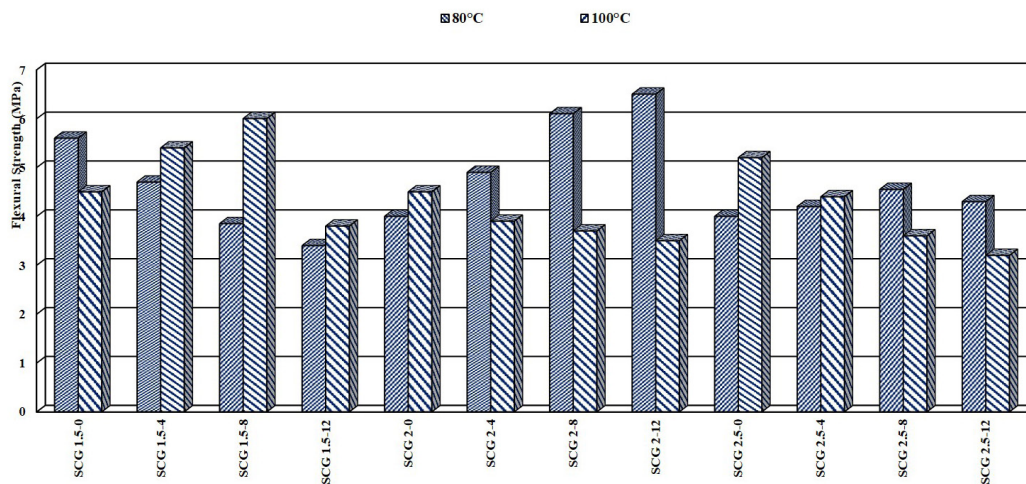


FIGURE 7. Flexural strength values of SCGs cured at 80 °C and 100 °C.

improvement of kinetic energy, resulting in stronger Al-Si-O networks of SCGs (37). Moreover, a higher NaOH concentration promoted higher strength at the early stages of the reaction. However, the strength of the activated geopolymer at the later stages might have decreased due to the excessive OH in the solution, causing the inhomogeneous morphology of the final products (44). SWM deteriorated the compressive strength at the highest alkali activator ratio in respect of curing temperature, which may be attributed to a weaker bond with the matrix of SWM as a result of incomplete geopolymerization controlled by the highest alkali activator ratio. Thus, SWM with the ability of microfibers to bridge micro-cracks did not help to achieve a higher load-carrying capability for SCGs. Moreover, the highest compressive strength for a lower curing temperature was obtained for SCG-2.5-0. A lower water content in the SCG series cured at 80 °C led to a higher alkalinity in Group II and Group III series compared to Group I series. Thus, the dissolution ratio of amorphous geopolymer would be higher in

Group II and Group III series, which accelerated the geopolymerization reaction (47). The replacement percentage of SWM did not have a positive effect on compressive strength due to a lower curing temperature for SCG-1.5, SCG-2, and SCG-2.5 samples. Considering the test results, the compressive strength values of SCG-1.5 cured at 100 °C increased up to 8% (including 8%) SWM content and decreased at 12%. In light of such information, it was determined that substituting SWM with FA in SCG-1.5 cured at 100 °C was critical for an 8% replacement level on the 28th day. The positive effect of SWM on compressive strength was explained by the filler effect of SWM in the matrix, resulting in a higher density in the microstructure considering the binder content, optimum curing temperature, and alkali activator ratio of SCGs. Upon comparing Group II, Group III, and Group I mixtures cured at 100 °C, the reason for the improvement in compressive strength of Group I mixtures may be supported by the addition of SWM that improved the microstructure of the geopolymer matrix owing to the mechanical inter-

locking of unreacted SWM molecules and connecting to the geopolymeric gel. However, an increase in the SWM percentage to 12% by mass in all groups for both curing temperatures increased the proportion of unreacted SWM molecules in the geopolymer matrix. Compared to Group I series, this situation could destroy the geopolymeric gel mesh and disrupt the matrix structure by decreasing compressive strength values. Another reason was that SWM partially disintegrated in the alkaline medium and the dissolution rate increased proportionally with alkalinity (25). Moreover, a higher compressive strength in SCG series mixtures can be explained by the fact that dissoluble calcium caused by SWM could react quickly with Si and Al to form the geopolymeric gel (2). Additionally, it was revealed that the strength loss due to the increased percentage of SWM was related to the increase in the amount of water needed for the other groups, except for Group I cured at 100 °C. The high aspect ratio (30:1) and high surface area of SWM caused a loss of workability, resulting in the need for water to obtain the aimed slump flow diameter of SCGs. Likewise, Patankar et al. (35) found that the excessive amount of water used during the polymerization of the sample did not make any positive contribution to strength characteristics. In addition, the presence of dissoluble silica affected the dissolution of FA, the reaction percentage of crystallization, and kinetics for different  $\text{Na}_2\text{SiO}_3/\text{NaOH}$  ratios. Silica causes strong Si gel formation, supporting the precipitation of big molecular types. Thus, silica is an important compound for the strength increment of the material with an improved density (48).

The flexural strength values of geopolymer mortars changed between 3.2-6.5 MPa, as shown in Figure 7. The highest flexural strength was obtained from SCG-2-12 cured at 80 °C, while SCG-2.5-12 cured at 100 °C had the lowest flexural strength. Similar to compressive test results, the increasing replacement percentages of SWM decreased flexural strength in Group I cured at 80 °C. This may be attributed to the lowest alkaline ratio controlling geopolymerization, which is responsible for the dissolution of solid fly ash particles. Thus, the degree of polymerization of the dissolved gel was affected by soluble silicates. Due to the weaker matrix of SCGs, the flexural strength of SCGs decreased with the increasing percentage ratio of SWM in Group I. Based on the observation from the test results, the improvement in the flexural strength of SCGs cured at 80 °C in Groups II and III can be explained by the fact that SWM could bind between microcracks (45, 46). Therefore, mechanical properties were improved by increasing the microfiber/matrix bond strength at the interface (47, 48). Studies in the literature have shown that the bond between wollastonite within a geopolymer matrix increases the flexural strength of SCGs with the increasing replacement percentages of SWM. If the strength of the geopolymer matrix based on geopolymerization is high, SWM with an acicular structure can attach to the geopolymer matrix. Thus, large

acicular SWM failed during loading, causing SCGs to be able to maintain their higher flexural strength (21). On the other hand, SWM partly disintegrated in the alkaline medium and finally fused to the geopolymeric gel, which strengthened the geopolymer matrix and improved the flexural properties of SCG-2-12 cured at 80 °C (21, 25). Similar to this study, it was stated that fibers could control the crack width by increasing the amount of absorbable energy and caused a greater increase in flexural strength than compressive strength values (49). However, as shown in Figure 7, replacing the geopolymer binder with SWM did not increase the flexural strength of Group II and III series mixtures cured at 100 °C. During the formation of geopolymers, the water evaporated from the matrix during the curing or drying periods left discontinuous nanopores in the matrix. Thus, it can be thought that the breakage of SWM could cause SCGs to be unable to resist their flexural strength at high curing temperatures. As a result, the crack-bridging effect was reduced by adding SWM fibers. On the other hand, SWM particles could be highly etched in SCG series mixtures due to their more alkaline medium. Thus, SWM could not fulfill its function as a fiber by reinforcing SCGs against bending, compared to mixtures cured at lower temperatures. These results were also supported by Bong and Nemattollahi (19).

Figure 8 present the ultrasonic pulse velocity (UPV) variations of SCGs on the 28th day for samples cured at different temperatures. The UPV values of SCGs changed in parallel with compressive strength. As seen in Figure 8, the UPV values of geopolymer mortars changed in the range of 2299-3524 m/s. The highest UPV value cured at 100 °C and the lowest UPV value cured at 80 °C were obtained from SCG-1.5-8 and SCG-1.5-12, respectively. UPV values improved in the mixtures cured at 100 °C with an alkaline ratio of 1.5. On the other hand, the increasing replacement percentages of SWM improved UPV values at a ratio of 5% and 6% in SCG-1.5-4 and SCG-1.5-8 compared to SCG-1.5-0 for Group I cured at 100 °C (without SCG-1.5-12). In case of SCG-1.5-12, the reason for deterioration may be the attenuation of the matrix bond in the interfacial transition zone of the excessive amount of SWM (15). The filler effect of SWM caused an increase in density in the microstructure for the transitional zone around the synthetic fiber, which was the reason for the denser matrix bound up to an 8% replacement percentage of SWM and provided the lack of continuity in pores (50, 51). Moreover, this development could have originated from the bond strength supported by the microfiber/matrix in the interfacial of SWM microfibers (52-54). Upon comparing the samples cured at 80 °C, it was found that the UPV values of Group I were lower than those of Groups II and III. It was thought that the reason for this was the weaker geopolymer matrix due to the insufficient amount of  $\text{Na}_2\text{SiO}_3/\text{NaOH}$ . However, it was determined that the mixtures in Group II had higher UPV values than those in Group III. The alkali content



and water ratio of Group II were found to be more suitable than those in Group III for sufficient geopolymer activation. Moreover, according to the classification of both, all the samples produced in this study can be considered as “medium” on the 28th day (55). Additionally, it can be said that the UPV values of SCGs exhibited a similar trend to the hardened bulk density values rather than their compressive and flexural strength values. Likewise, Xu *et al.* (56) reported that some of the ultrasonic wave energy was lost due to the porous structure during the test, while the UPV measurement of samples with low density and high porosity was reduced.

The dynamic modulus of elasticity is directly based on the time controlled by the voids in the concrete/geopolymer, which is necessary to move ultrasonic pulse waves through the sample (57). Furthermore, the deformation behavior of structural elements can be observed by DME while being subjected to a load (58). It is reported that the reduction of density results in a lower time, which in turn decreases speed (km/s) (57). Figure 9 indicate DME as a function of the hardened bulk density of SCGs and ultrasonic pulse velocity (m/s). As

seen in Figure 9, the hardened bulk density of SCGs affected DME. Similar to the results of the study by Alnahhal *et al.* (57), the voids of the sample obstructed the movement of ultrasonic pulse waves, which increased the time required to pass the ultrasonic pulse wave. The filler effect of SWM, the formation of bond strength supported by the microfiber/matrix in the interfacial of SWM microfibers, and the sufficient alkali content and water ratio improved UPV measurements, which in turn increased DME. The highest DME values were detected in Groups I and III cured at 100 °C, which were 22.37 GPa and 22.01 GPa, respectively. It can be concluded that the hardened bulk density, UPV, replacement percentages of SWM, and alkali ratio determined the range of DME for SCGs.

### 3.4. Water sorptivity coefficient

Water sorptivity coefficient values were obtained from the experiments performed on the 28th day

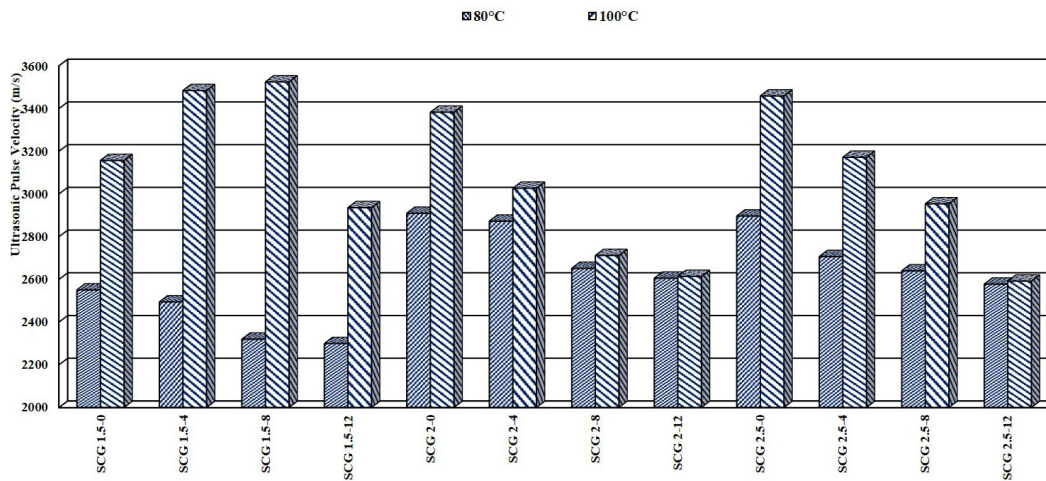


FIGURE 8. Ultrasonic pulse velocity values of SCGs cured at 80 °C and 100 °C.

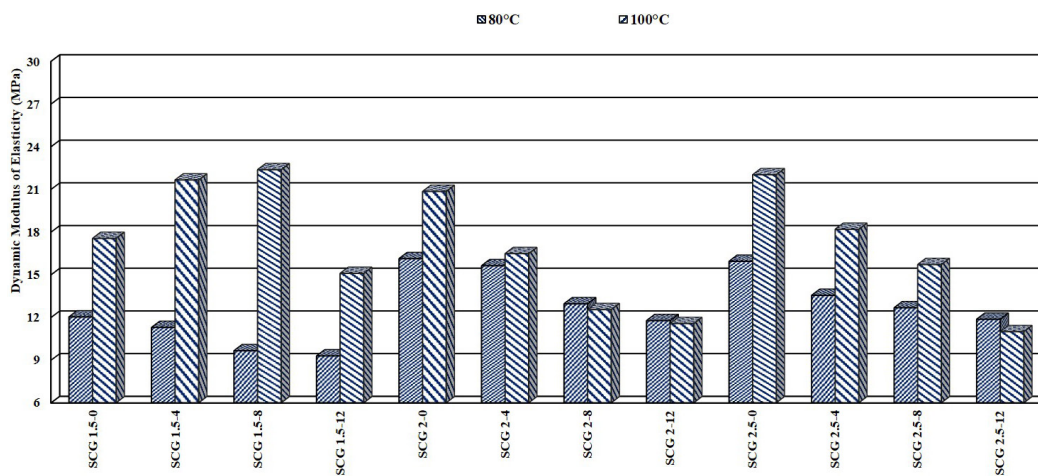


FIGURE 9. Dynamic modulus of elasticity (MPa) values of SCGs cured at 80 °C and 100 °C.

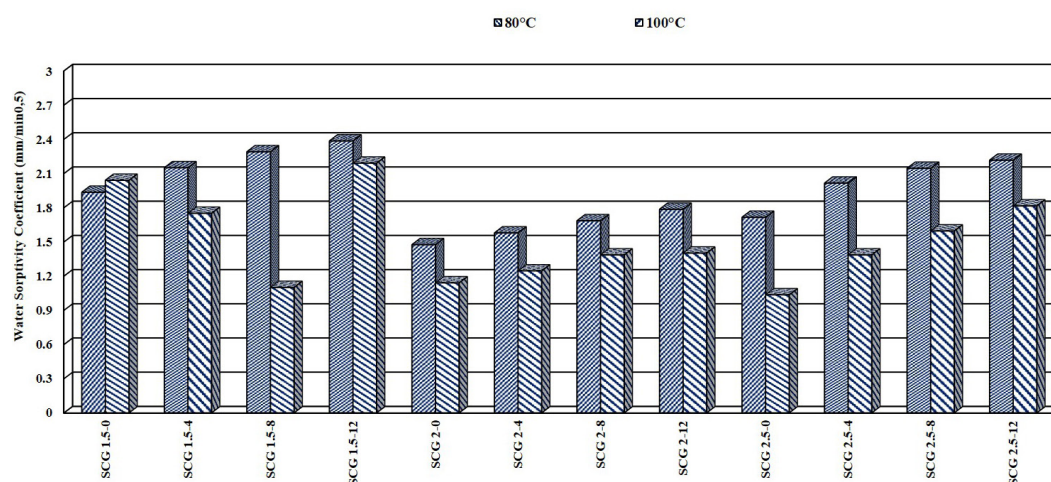


FIGURE 10. Water sorptivity coefficient values of SCGs cured at 80 °C and 100 °C.

of SCGs produced under different curing conditions and are presented in Figure 10. According to the test results, the water sorptivity coefficient values of geopolymer mortars changed in the range of 1.10-2.38 mm/min<sup>0.5</sup>, respectively. The highest water sorptivity coefficient was obtained from SCG-1.5-12 cured at 80 °C, whereas SCG-1.5-8 cured at 100 °C had the lowest water sorptivity coefficient. As seen from Figure 10, the water sorptivity coefficient increased with the increasing percentage of SWM in SCGs cured at 80 °C for all groups and 100 °C, except for Group I, respectively. Considering the test results for Group I mortars cured at 100 °C, when the amount of SWM increased, the water sorptivity coefficient values of SCGs decreased on the 28th day, and this development continued to 8% of SWM (including 8%). Hence, the compactness of the microstructure with curing the geopolymer at a high temperature can be attributed to a reduction in pores via the positive filler effect of SWM (47). Thus, a pore discontinuity could be provided with the formation of the pore structure of SWM in the geopolymer system, which liquids cannot attain at normal pressures (50). However, using SWM at a 12% replacement percentage deteriorated the mechanical performance of SCGs. The impairment of SCG-1.5-12 cured 100 °C in Group I can be explained by the weakening of the matrix bond in the interfacial transition zone of SWM (51). Additionally, this value increased in Group I cured at 80 °C due to the presence of such pores formed as a result of the evaporation of the free water not included in geopolymerization during the curing period from the samples. Thus, higher water usage for the aimed slump flow diameter of SCGs due to the high aspect ratio (30:1) and high surface area of SWM caused a loss of workability, which adversely affected mechanical properties. As a result, the gaps created due to more water leaving the mortar after curing caused an increment in the water sorptivity coefficient values of SCGs. In addition to these, it is thought that choosing

a high molarity of NaOH causes a decrease in capillarity. Furthermore, this may be related to the gel's concentration since the increasing temperature causes the gel to bind denser. Moreover, water sorptivity coefficient values are generally related to the values of apparent porosity. Therefore, water sorptivity coefficients decreased with the reduction in porosity due to increasing unit volume weights (7).

#### 4. CONCLUSIONS

In this study, SCGs incorporating SWM were designed as a new construction material using alkali activators under different curing conditions. Thus, the effect of SWM on the fresh and hardened state performance of SCGs was investigated in terms of testing parameters, such as the replacement percentage of SWM with FA, different alkali activator ratios and curing temperatures. The following results can be drawn:

The increased interlocking effect due to the needle-like structure of SWM reduced the workability of the mixture. Hence, more water must be used for the desired workability.

When SWM was used instead of FA as a filler, the reason for the decrease in hardened bulk density was an increased void ratio because of the water leaving the sample during geopolymerization.

It was determined that the dry specific gravity values of SCGs were in the range of 1.73-1.89, apparent specific gravity values changed between 2.33-2.51, and saturated dry surface specific gravity values varied between 2.00-2.12.

To obtain the same workability, an increase in the liquid-to-solid ratio has critical implications since it leads to slower polycondensation reactions. Moreover, the porosity rate of SCGs increased due to the formation of several networks at the highest curing temperature.

The highest compressive strength was obtained as 28.9 MPa from SCG-1.5-8 cured at 100 °C, while SCG-1.5-12 cured at 80 °C had the lowest compressive strength found as 12.8 MPa. Thus, high curing temperatures contributed to forming a denser matrix. Additionally, the increased quantity of unreacted wollastonite particles in the geopolymer matrix due to the increase in the SWM content of 12% by mass caused a lower compressive strength. This situation led to a weaker matrix with a lower compressive strength.

The flexural strength values of geopolymer mortars changed between 3.2-6.5 MPa. The improvement in the flexural strength of Groups II and III cured at 80 °C could be explained by the fact that SWM was partially disintegrated in the alkaline medium and finally bound to the geopolymeric gel, increasing the microfiber/matrix bond strength at the interface. However, SWM did not further increase the flexural strength values of Groups II and III cured at 100 °C. The water evaporation from the matrix during the curing periods left discontinuous nanopores in the matrix, which caused SCGs to be unable to resist their flexural strength.

The UPV values of geopolymer mortars changed in the range of 2299-3524 m/s. The UPV values of SCGs showed a similar trend to the hardened bulk density values rather than their compressive and flexural strength values. The highest dynamic modulus of elasticity values were detected in Groups I and III cured at 100 °C, which were 22.37 GPa and 22.01 GPa, respectively. It can be concluded that the hardened bulk density, UPV, replacement percentages of SWM, and alkali ratio determined the range of dynamic modulus of elasticity for SCGs.

The highest water sorptivity coefficient values of the geopolymer mortars cured at 80 °C were obtained from SCG-1.5-12 (2.38 mm/min<sup>0.5</sup>), whereas SCG-1.5-8 cured at 100 °C had the lowest water sorptivity coefficient (1.10 mm/min<sup>0.5</sup>). The water sorptivity coefficient values of SCGs decreased with the increasing SWM percentage since this special filler fiber reduced pores by improving the microstructure of the geopolymer matrix in SCG 1.5 (Group I) cured at 100 °C.

In this study, SWM produced with waste calcite and quartz sand can be used as an inert material instead of a binder. Additionally, the production of fly ash-based SCGs can contribute to the sustainable environment without more energy consumption for structural members. Thus, it can be concluded that this study on fly ash-based SCGs incorporating synthetic wollastonite microfibers designed in accordance with the standards is an important breakthrough in the utilization of waste materials.

#### AUTHOR CONTRIBUTIONS:

Conceptualization: H.Ö. Öz. Data curation: H.Ö. Öz, D. Ünsal. Formal analysis: H.Ö. Öz. Funding acquisition: H.Ö. Öz,

D. Ünsal. Methodology: H.Ö. Öz. Project administration: H.Ö. Öz. Resources: H.Ö. Öz. Software: H.Ö. Öz. Supervision: H.Ö. Öz. Validation: H.Ö. Öz. Visualization: H.Ö. Öz. Roles/Writing, original draft: H.Ö. Öz, D. Ünsal. Writing, review & editing: H.Ö. Öz, D. Ünsal.

#### REFERENCES

- Demie, S.; Nuruddin, M.F.; Shafiq, N. (2013) Effects of micro-structure characteristics of interfacial transition zone on the compressive strength of self-compacting geopolymer concrete. *Constr. Build. Mater.* 41, 91-98. <https://doi.org/10.1016/j.conbuildmat.2012.11.067>.
- Lee, W.K.W.; Van Deventer, J.S.J. (2002) The effect of ionic contaminants on the early-age properties of alkali-activated fly ash-based cements. *Cem. Concr. Res.* 32 [4], 577-584. [https://doi.org/10.1016/S0008-8846\(01\)00724-4](https://doi.org/10.1016/S0008-8846(01)00724-4).
- McDonald, M.; Thompson, J. (2005) Sodium silicate: A binder for the 21st century, The PQ Corporation. Industrial Chemicals Division.
- Hardjito, D.; Rangan, B.V. (2005) Development and properties of low-calcium fly ash based geopolymer concrete. Research Report GC 1. 1-94.
- Abdullah, M.M.A.B.; Kamarudin, H.; Khairul Nizar, I.; Bnhussain, M.; Zarina, Y.; Rafiza, A.R. (2012) Correlation between Na<sub>2</sub>SiO<sub>3</sub>/NaOH ratio and fly ash/alkaline activator ratio to the strength of geopolymer. *Adv. Mat. Res.* 341-342, 189-193 <https://doi.org/10.4028/www.scientific.net/AMR.341-342.189>.
- Sanni, S.H.; Khadiranaikar, R.B. (2013) Performance of alkaline solutions on grades of geopolymer concrete. *IJRET.* 366-371. <http://doi.org/10.15623/ijret.2013.0213069>.
- Kurklu, G.; Gorhan, G. (2019) Investigation of usability of quarry dust waste in fly ash-based geopolymer adhesive mortar production. *Constr. Build. Mater.* 217, 498-506. <https://doi.org/10.1016/j.conbuildmat.2019.05.104>.
- Joseph, B.; Mathew, G. (2012) Influence of aggregate content on the behaviour of fly ash based geopolymer concrete. *Scientia Iranica.* 19 [5], 1188-1194. <https://doi.org/10.1016/j.scientia.2012.07.006>.
- Petermann, J.C.; Saeed, A.; Hammons, M.I. (2010) Alkali-activated geopolymers: a literature review. Air force research laboratory materials and manufacturing directorate, 88ABW-2012-2030. Retrieved from: <https://apps.dtic.mil/sti/pdfs/ADA559113.pdf>.
- Silva, F.J.; Mathias, A.F.; Thaumaturgo, C. (1999) Evaluation of the fracture toughness in poly (sialate-siloxo) composite matrix. Proceedings of the Geopolymer International Conference (Geopolymer '99). 97-106.
- Virta, R.L. (2011) Wollastonite, In Minerals yearbook, U.S. Geological Survey. Retrieved from: <http://minerals.usgs.gov/minerals/pubs/commodity/wollastonite/myb1-2010-wolla.pdf>.
- Kogel, J.E.; Trivedi, N.C.; Barker, J.M.; Krukowski, S.T. (2006) Industrial minerals & rocks, 7th ed. Society for Mining, Metallurgy and Exploration.
- Virta, R.L. (1999) Wollastonite. US Geological Survey Mineral Yearbook.
- Akkaya, Y.; Kesler, Y.E. (2012) Mikro kalsit katkısının betonun işlenebilirliğine, mekanik özelliklerine ve dayanıklılığına etkisi. *IMO Teknik Dergi.* 384, 6051-6061.
- Oz, H.O.; Güneş, M. (2021) The effects of synthetic wollastonite developed with calcite and quartz on high performance mortars. *Struct. Concr.* 22 [S1], E257-E272. <https://doi.org/10.1002/suco.201900520>.
- Yücel, H.E.; Özcan, S.; (2019) Strength characteristics and microstructural properties of cement mortars incorporating synthetic wollastonite produced with a new technique. *Constr. Build. Mater.* 223, 165-176. <https://doi.org/10.1016/j.conbuildmat.2019.06.195>.
- Oz, H.O.; Gunes, M. (2018) Wollastonit katkıli yüksek performanslı harçların mekanik ve durabilite özellikleri. Graduate Theses and Dissertations.
- Kalla, P.; Rana, A.; Chad, Y.B.; Misra, A.; Csetenyi, L. (2015) Durability studies on concrete containing wollastonite. *J. Clean. Pro.* 87, 726-734. <https://doi.org/10.1016/j.jclepro.2014.10.038>.



19. Bong, S.H.; Nematollahi, B.; Xia, M.; Nazari, A.; Sanjayan, J. (2020) Properties of one-part geopolymer incorporating wollastonite as partial replacement of geopolymer precursor or sand. *Mater. Letters*. 263, 127263. <https://doi.org/10.1016/j.matlet.2019.127236>.
20. Ling, Y. (2018) Proportion and performance evaluation of fly ash based geopolymer and its application in engineered composites. *Graduate Theses and Dissertations*. <https://doi.org/10.31274/etd-180810-6028>.
21. Nurjaya, D.M.; Astutiningsih, S.; Zulfia, A. (2015) Thermal effect on flexural strength of geopolymer matrix composite with alumina and wollastonite as fillers. *Int. J. Technol.* 6, 462–470. <https://doi.org/10.14716/ijtech.v6i3.1441>.
22. Ransinchung, G.D.; Kumar, B. (2010) Investigations on pastes and mortars of ordinary portland cement admixed with wollastonite and microsilica. *J. Mater. in Civil Eng.* 22 [4]. [https://doi.org/10.1061/\(ASCE\)MT.1943-5533.0000019](https://doi.org/10.1061/(ASCE)MT.1943-5533.0000019).
23. Nuruddin, M.F.; Samuel, D.; Nasir, S. (2011) Effect of mix composition on workability and compressive strength of self-compacting geopolymer concrete. *Can. J. Civil Eng. NRC Res. Press.* 38 [11], 1196–203. <https://doi.org/10.1139/11-077>.
24. Memon, F.A.; Nuriddin, M.F.; Demie, S.; Shafiq, N. (2011) Effect of curing conditions on strength of fly-ashed based self-compacting geopolymer concrete. *IJCEE* 5 [8], 342-345. <https://doi.org/10.5281/zenodo.1070949>.
25. Yip, C.K.; Lukey, G.C.; Provis, J.L.; Van Deventer, J.S. (2008) Effect of calcium silicate sources on geopolymerisation. *Cem. Concr. Res.* 38 [4], 554–564. <https://doi.org/10.1016/j.cemconres.2007.11.001>.
26. EFNARC F. (2002) Specification and guidelines for self-compacting concrete, European federation of specialist construction chemicals and concrete system.
27. Matsimbe, J.; Dinka, M.; Olukanni, D.; Musonda, I. (2022) Geopolymer: a systematic review of methodologies. *Materials*. 15, 6852. <https://doi.org/10.3390/ma15196852>.
28. ASTM C642-13 (2013) Standard test method for density, absorption, and voids in hardened concrete, West Conshohocken PA.
29. ASTM C348-14 (2017) Standard test method for flexural strength of hydraulic-cement mortars, Annual Book of ASTM Standards.
30. ASTM C349-14 (2017) Standard test method for compressive strength of hydraulic-cement mortars (using portions of prisms broken in flexure), Annual Book of ASTM Standards.
31. ASTM C597-16 (2016) Standard Test Method for Pulse Velocity Through Concrete, Annual Book of ASTM Standards.
32. Haseli, M.; Layeghi, M.; Hosseinabadi, H.Z. (2020) Evaluation of modulus of elasticity of date palm sandwich panels using ultrasonic wave velocity and experimental models. *Measurement*. 149, 107016. <https://doi.org/10.1016/j.measurement.2019.107016>.
33. ASTM C1585-20 (2020) Standard Test Method for Measurement of Rate of Absorption of Water by Hydraulic-Cement Concretes. West Conshohocken, PA: ASTM International.
34. Tatnall, P.C. (2006) Fiber-reinforced concrete. *E-Publishing Inc.* 578–590.
35. Patankar, S.V.; Jamkar, S.S.; Ghugal, Y.M. (2012) Effect of sodium hydroxide on flow and strength of fly ash based geopolymer mortar. *J. Struct. Eng.* 39 [1], 7–12.
36. Atabey, I.I. (2017) F sınıfı uçucu küllü geopolimer harcının durabilite özelliklerinin araştırılması. Graduate Theses and Dissertations.
37. Öz, H.Ö.; Doğan-Sağlamtimur, N.; Bilgil, A.; Tamer, A.; Günaydin, K. (2021) Process development of fly ash-based geopolymer mortars in view of the mechanical characteristics. *Materials*. 29, 14 [11], 1-22. <https://doi.org/10.3390/ma14112935>.
38. Renumathi, M.; Mukesh, P.; Balamurugan, P. (2020) A state of art on geopolymer concrete. *Adalya J.* 9 [1], 372-378.
39. Zuhua, Z.; Xiao, Y.; Huajun, Z.; Yue, C. (2009) Role of water in the synthesis of calcined kaolin based geopolymer. *Appl. Clay Sci.* 43, 218–223. <https://doi.org/10.1016/j.clay.2008.09.003>.
40. Prud'homme, E.; Joussein, E.; Peyratout, C.; Smith, A.; Rossignol, S. (2010) Consolidated geo-materials from sand or industrial waste. *Ceram. Eng. Sci.* 30, 314–324. <https://doi.org/10.1002/9780470584262.ch29>.
41. Kovalchuk, G.; Fernandez-Jimenez, A.; Palomo, A. (2017) Alkali activated fly ash: effect of thermal curing conditions on mechanical and microstructural development-Part II. *Fuel*. 86, 315-22. <https://doi.org/10.1016/j.fuel.2006.07.010>.
42. Lin, K.; Chang, J.; Chen, G.; Ruan, M.; Ning, C. (2007) A simple method to synthesize single-crystalline  $\beta$ -wollastonite nanowires. *Mater. Sci.* 300 [2], 267-271. <https://doi.org/10.1016/j.jcrysgro.2006.11.215>.
43. Lai, M.; Binhowimal, S.; Hanžič, L.; Wang, Q.; Ho, J. (2020) Dilatancy mitigation of cement powder paste by pozzolanic and inert fillers. *Struct. Concr.* 21 [4], 1-17. <https://doi.org/10.1002/suco.201900320>.
44. Khale, D.; Chaudhary, R. (2007) Mechanism of geopolymerization and factors influencing its development. *J. Mater. Sci.* 42, 729-746. <https://doi.org/10.1007/s10853-006-0401-4>.
45. Nikonova, N.S.; Tikhomirova, I.N.; Belyakov, A.V.; Zakharov, A.I. (2003) Wollastonite in silicate matrices. *Glass Ceramics*. 60, 342-346. <https://doi.org/10.1023/B:GLAC.0000008241.84600.f9>.
46. Dey, V.; Kachala, R.; Bonakdar, A.; Mobasher, B. (2015) Mechanical properties of micro and sub-micron wollastonite fibers in cementitious composites. *Constr. Build. Mater.* 82, 351-359. <https://doi.org/10.1016/j.conbuildmat.2015.02.084>.
47. Duxson, P.; Fernández-Jiménez, A.; Provis, J.L.; Lukey, G.C.; Palomo, A.; Van Deventer, J.S. (2007) Geopolymer technology: the current state of the art. *J. Mater. Sci.* 42 [9], 2917–2933. <https://doi.org/10.1007/s10853-006-0637-z>.
48. Zuda, L.; Pavlik, Z.; Rovnanikova, P.; Bayer, P.; Cerny, R. (2006) Properties of alkali activated aluminosilicate material after thermal load. *Int. J. Thermophys.* 27 [4], 1250-1263. <https://doi.org/10.1007/s10765-006-0077-7>.
49. Hughes, B.P. (1981) Design of prestressed fiber reinforced concrete beams for impact. *ACI Materials Journal*. 78, 276-281.
50. Mathur, R.; Misra, A.K.; Goel, P. (2007) Influence of wollastonite on mechanical properties of concrete. *J. Sci. Ind. Res.* 66, 1029–1034.
51. Wahab, M.A. Latif, I.A.; Kohail, M.; Almasry, A. (2017) The use of wollastonite to enhance the mechanical properties of mortar mixes. *Constr. Build. Mater.* 152, 304–309. <https://doi.org/10.1016/j.conbuildmat.2017.07.005>.
52. Soliman, A.M.; Nehdi, M.L. (2014) Effects of shrinkage reducing admixture and wollastonite microfiber on early-age behaviour of ultrahigh performance concrete. *Cem. Concr. Compos.* 46, 81–89. <https://doi.org/10.1016/j.cemconcomp.2013.11.008>.
53. Banthia, N.; Sheng, J. (1996) Fracture toughness of micro-fiber reinforced cement composites. *Cem. Concr. Compos.* 18 [4], 251–269. [https://doi.org/10.1016/0958-9465\(95\)00030-5](https://doi.org/10.1016/0958-9465(95)00030-5).
54. Hameed, R.; Turatsinze, A.; Duprat, F.; Sellier, A. (2009) Metallic fiber reinforced concrete: Effect of fiber aspect ratio on the flexural properties. *ARPN J. Eng. Appl. Sci.* 4, 67–72.
55. Malhotra, V.M. (1976) Testing hardened concrete: nondestructive methods. ACI Monograph No.9.
56. Xu, S.; Malik, M.A.; Qi, Z.; Huang, B.; Li, Q.; Sarkar, M. (2018) Influence of the PVA fibers and SiO<sub>2</sub> NPs on the structural properties of fly ash based sustainable geopolymer. *Constr. Build. Mater.* 164, 238–245. <https://doi.org/10.1016/j.conbuildmat.2017.12.227>.
57. Alnahhal, A.M.; Alengaram, U.J.; Yusoff, S.; Singh, R.; Radwan, M.K.H.; Deboucha, W. (2021) Synthesis of sustainable lightweight foamed concrete using palm oil fuel ash as a cement replacement material. *J. Build. Eng.* 35, 102047. <https://doi.org/10.1016/j.jobte.2020.102047>.
58. Gupta, T.; Siddique, S.; Sharma, R.K.; Chaudhary, S. (2017) Effect of elevated temperature and cooling regimes on mechanical and durability properties of concrete containing waste rubber fiber. *Constr. Build. Mater.* 137, 35–45. <https://doi.org/10.1016/j.conbuildmat.2017.01.065>.